

Evaluation of Abrasive Wear in UNS S32101 and S32750 Duplex Stainless Steels Submitted to Friction Stir Processing

Igor Jordão Marques^a, Flávio José da Silva^b, Thiago Santana de França^a, Guilherme Gadelha de Sousa^a,

Tahiana Francisca da Conceição Hermenegildo^b, Tiago Felipe de Abreu Santos^{a*}

^a Universidade Federal de Pernambuco, Departamento de Engenharia Mecânica, Av. da Arquitetura, s/n, Cidade Universitária, CEP: 50750-550, Recife, PE, Brasil

^b Universidade Federal do Rio Grande do Norte, Departamento de Engenharia Mecânica, Anel Viário Contorno do Campus, s/n, Capim Macio, CEP: 59078-970, Natal, RN, Brasil

Received: December 8, 2018; Revised: December 23, 2019; Accepted: January 12, 2020

Duplex stainless steels are largely applied in petrochemical industries due to their high corrosion resistance and mechanical performance. Their applicability also requires a great wear resistance, which can be enhanced by friction stir processing (FSP), a surface hardening technique. In this work, FSP is utilized to process surfaces of UNS S32101 and UNS S32750. The materials were analyzed by EBSD in order to determine grain size and phase fraction. Microhardness tests were used to verify and compare the shifting of hardness values from 296 ± 8 to 314 ± 11 HV_{0.2/15} and from 323 ± 8 to 350 ± 8 HV_{0.2/15} for UNS S32101 and S32750, respectively. Abrasion tests were executed to study the wear behavior of both processed and unprocessed alloys. Abrasion tests indicated that the hardening by FSP promoted decrement of abrasive wear resistance. Volumetric loss increased after FSP, from 52.1 ± 0.5 to 53 ± 2 mm³, for UNS S32101, and from 50 ± 2 to 56.3 ± 0.3 mm³ for UNS S32750. Tensile tests results were fitted to Hollomon's equation in order to identify mechanical properties and tendencies of strain hardening. SEM images were used to classify the wear micromechanisms acting on the samples. The results suggest that FSP can promote modifications of wear mechanisms and these changes can be correlated to the alloys' microstructure.

Keywords: Duplex stainless steels, friction stir processing, abrasive wear, hardening, microploughing, microcutting.

1. Introduction

Duplex stainless steels (DSS's) stand out among stainless steels due to their excellent mechanical strength, great corrosion resistance and weldability. These properties are a consequence from their biphasic microstructure composed of austenite and ferrite in a nearly equivalent volumetric fraction^{1,2}. DSS's are mainly applied in gas and petrochemical industries, and are frequently a necessary choice for offshore components and projects^{3,4}.

Particularly, during oil and gas extraction, a mixture of fluids with fine abrasive and particulates is transported within the pipe system. These elements present in crude oil are prone to cause processes such as wear and tribocorrosion⁵. Additionally, the fluid's chemical mixture offers a great risk of corrosion owing to the transport of chlorides, sulfides and organic compounds⁵. The combination of substances found in crude oil requires specifications which are found in materials with high corrosion resistance. However, the presence of the fine sand particulates in the mixture causes tribological processes that can harm the structures of materials exposed to it. Then, it is comprehensible that the material must have great wear resistance, as well as good corrosion resistance. Especially in the case of passivable materials such as DSS'S, when the passive layer is attacked by electrochemical and mechanical effects concomitantly, the degradation of the

material is intensified, being damaged by the tribological wear and, consequently, allowing corrosive action into the metallic substrate.

The wear processes can be divided into four main forms: abrasive wear, adhesive wear, tribochemical wear and contact fatigue. Abrasive wear can be defined as the removal of material caused by hard particles or forced protuberances against and along a solid surface⁶. Abrasive wear is one of the most severe modes of wear, generally causing greater superficial damage or loss of surface material⁷. The mechanisms of abrasive wear may involve both plastic deformation and brittle fracture⁶. During abrasion, two different basic wear modes occur due to plastic deformation: microploughing and microcutting. The microploughing occurs when the abrasive particles mainly cause deformation of the material, in a way that the material removed from the groove is distributed on the groove's adjacencies. The effective material removal during microploughing action occurs when several particles act on neighboring regions, affecting the adjacencies of grooves, which were formed previously, and then promoting microfatigue of the material⁶. Differently, microcutting occurs when the deformation promoted by hard abrasive particles is sufficiently intense to cause fracture of the material removed from groove⁶. Some variables are fundamental and strongly influence the rate of abrasive wear: the hardness of the materials in abrasive contact, the abrasive particles' geometry, the loading intensity and the distance of the wear path⁶.

*e-mail: tiago.felipe@ufpe.br

Surface processing techniques are important tools in tribology. Such methods may consist of thermomechanical processing, surface coatings, or thermochemical processing, for example. For duplex stainless steels, there are studies showing the success of using thermal treatments for increasing abrasion resistance ⁸, increasing corrosion resistance and slip wear via laser shock peening ⁹, and applying friction stir processing (FSP) for improving cavitation resistance ¹⁰. Surface treatment by FSP is derived from the friction stir welding (FSW) process ^{11,12}. FSP occurs mainly through the contact of a rotating tool, composed of a shoulder and pin, that is plunged with an axial force in the workpiece, generating heat by friction and deformation. In this process the microstructure of the material undergoes severe hot plastic deformation, resulting in a ultra-fine grains microstructure caused by recrystallization and recovery processes ¹³. Advantages of employing FSP can span from microstructure homogenization, production of superplastic materials and special alloys, porosity reduction in casting alloys, to crack repairing ¹⁴. Additionally, FSP can be applicable using a pre-deposited material in order to manufacture composites (friction stir alloying) ¹⁵, and to coat surfaces using a consumable tool (friction surfacing) ¹⁶. Recently, this manufacturing process has also improved technologically with the addition of ultrasound waves. This coupled system is promised to reduce processing forces, increase process speed and reduce manufacturing costs ¹⁷⁻¹⁹. Apart their different technological purpose, FSP and FSW are correlated processes, as input parameters and phenomena observed during the execution of both manufacturing procedures can be linked to produce similar metallurgical results ^{11,12,14,20}. The friction stir welding process was already promising for the welding of duplex stainless steels ²¹⁻²⁴, since this process allowed to obtain welded joints with superior mechanical properties to those obtained by conventional welding, with absence of secondary deleterious phases, despite the welds obtained with this process present higher propensity to formation of these phases after the joining ²⁵. Besides, this process tends to avoid the excessive formation of ferrite, a recurring problem in the thermo-mechanical processing of DSS's ^{24,26}. The success in the usage of FSP to improve cavitation resistance in duplex and austenitic stainless steels ^{10,27} and abrasive wear resistance in austenitic stainless steel ²⁸ has been reported. However, there are no records in the literature on the effects of FSP on abrasive wear resistance in duplex stainless steels. As one can perceive, abrasion resistance in duplex stainless steels is an important requirement for some industrial applications. This work aims to investigate the effect of FSP on abrasive wear resistance in duplex stainless

steels and provide a contribution for the understanding of abrasive wear resistance of FSP samples.

2. Experimental Procedure

In this study, 6 mm sheets of duplex stainless steels UNS S32101 (EN 1.4162) and UNS S32750 (EN 1.4410), provided by Outokumpu, were used in the state of "as-received" and processed by Friction Stir Processing using a Transformation Technologies RM-1a FSP machine. Table 1 shows the alloy's chemical composition. Processing direction was perpendicular to the workpiece's rolling direction, using a non-consumable PCBN-40% -W-Re tool, with a 6 mm length and 8 mm width pin and a 25 mm diameter concave shoulder. Processing parameters were: rotation speed of 200 rpm, longitudinal speed of 100 mm.min⁻¹ and axial force of 37 kN.

Electron backscattered electron diffraction (EBSD) analysis were performed on a Philips FEG XL 30 SEM for microstructural characterization. 300 x 300 μm with 1 μm step and 100 x 100 μm with 0.1 μm step EBSD maps were acquired to analyze the material as received and the friction stir processed material, respectively. The oriented image maps were indexed with TSL OIM Analysis software and the analysis of EBSD data were performed using MTEX toolbox ²⁹.

Vickers microhardness maps were performed with a load of 200 gf applied for 15 s (HV_{0.2/15}) on each indentation. Tensile tests were performed according with ASTM A370 standard. Rubber wheel abrasion tests were performed according with ASTM G65 using 130 N applied load, 320 g/min mass flow of abrasive particles and 200 rpm rubber wheel speed with 25 x 76 x 6 mm samples. The abrasive particles were Brazilian Standard No. 100 sand - SiO₂. The worn surfaces were characterized by scanning electron microscopy to identify the wear mechanisms. The Figure 1 presents a schematic of the rubber wheel abrasometer built at UFPE and calibrated with several others Brazilian laboratories (interlaboratory experiments), before the final experiments have performed.

3. Results and Discussion

3.1 Microstructure analysis

Figure 2 and Figure 3 shows average grain size maps of the UNS S32101 and S32750, respectively, before and after FSP. The FSP resulted in a biphasic austenite-ferrite microstructure of equiaxial grains, with no formation of secondary phases. In comparison to the original microstructure, refined grains were also present. Table 2 shows the EBSD results for grain size and volumetric fraction of ferrite

Table 1. Chemical composition (% by weight) of duplex stainless steels UNS S 32101 and UNS S32750.

UNS	ISO	C	Si	Mn	Cr	Ni	Mo	Cu	N	P	S
S32101	1.4162	0.02	0.70	5.13	21.4	1.62	0.21	0.28	0.22	0.023	0.001
S32750	1.4410	0.02	0.25	0.78	24.9	6.88	3.79	0.34	0.26	0.023	0.001

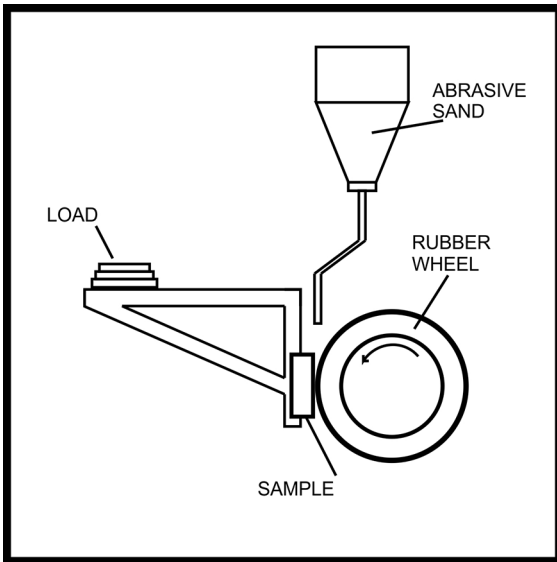


Figure 1. Schematic of the rubber wheel abrasion test.

before and after FSP. EBSD quantitative measurements were conducted in the samples processed by FSP, in the center of the processed region (stirred zone). The results indicated that the surface treatment tended to maintain the ferrite volume fraction originally present in the untreated

material, approximately 51.5% and 42.5% for UNS S32101 and S32750, respectively. In addition, the average grain size of both phases was reduced by at least 50% of the initial value. Figure 4 shows histograms of mean grain size of UNS S32101 and S32750 before and after frictions stir processing. The results suggested that FSP was more effective when processing the UNS S32750, once this material developed higher fractions of small grain sizes when compared to UNS S32101. The grain size distribution indicated that FSP promoted a microstructure refinement, producing finer grains with a higher volumetric fraction, and thus reducing the maximum average grain size. In the processed samples, there was an increase in grain size dispersion. However, this effect occurred mainly due to growth of the finer grains' fraction. It was noted that the greater dispersion of grain size was more significant in the ferrite than in the austenite. This behavior is caused by ferrite's diverse recovery mechanisms during FSP: initially, this phase presents a dynamic recovery, which then evolves to recrystallization. It is worth mentioning that FSP did not promote strain hardening of the workpiece, as microstructural modifications promoted by this process are due to recrystallization phenomena¹³. A more detailed discussion about the microstructural development of DSS's on FSP was published previously by Santos et al.¹³.

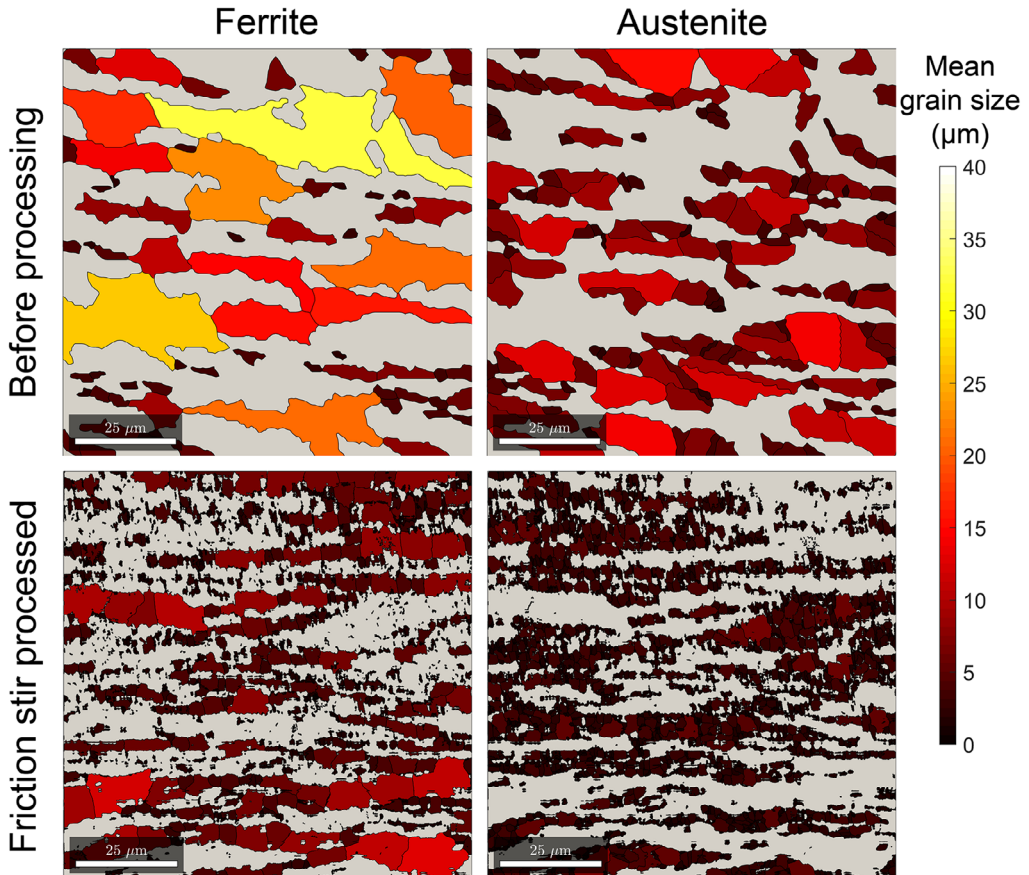


Figure 2. Average grain size maps obtained from EBSD analysis of UNS S32101 before and after FSP.

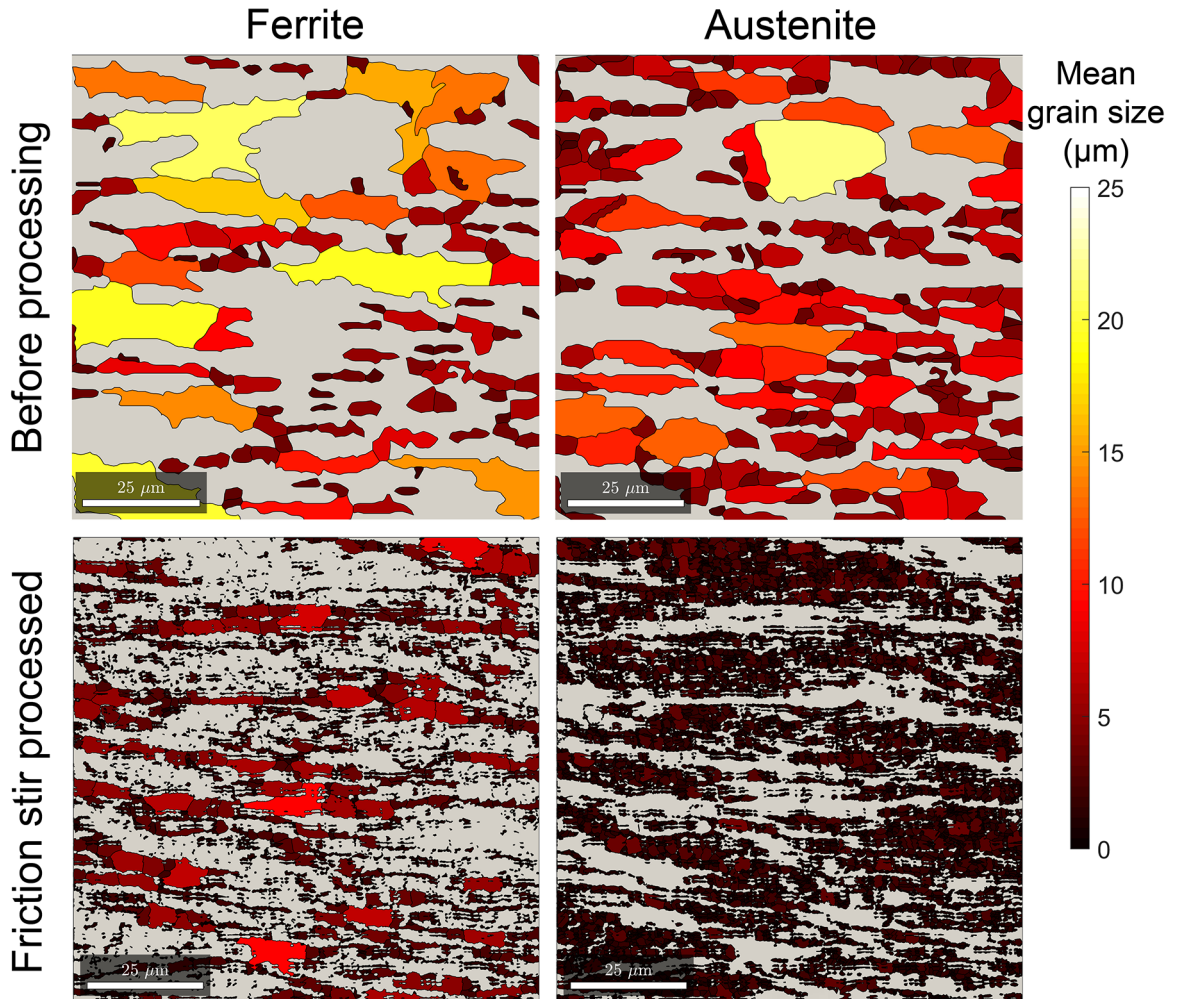


Figure 3. Average grain size maps obtained from EBSD analysis of UNS S32750 before and after FSP

Table 2. EBSD measures for grain sizes and volumetric fraction of ferrite from UNS S32101 and UNS S32750 alloys before and after FSP.

Steel alloy	Condition	Average Grain size (μm)		Ferrite volumetric fraction (%)
		Ferrite	Austenite	
UNS S32101	Before FSP	11.9 ± 1.1	12.9 ± 0.5	51.0
	FSP	5.0 ± 0.2	2.5 ± 0.1	52.1
UNS S32750	Before FSP	7.3 ± 0.4	7.1 ± 0.4	43.6
	FSP	1.8 ± 0.1	1.1 ± 0.1	42.5

3.2 Mechanical Performance Evaluation

3.2.1 Microhardness

Figure 5 shows the schematic of the regions where the microhardness measures were conducted. Microhardness profiles and maps were computed on cross sections (Figure 6) and surfaces (Figure 7) of FSP samples. Figure 6 shows the hardness maps obtained by the microhardness tests on the cross sections of processed samples. Cross section maps showed an overall increase in hardness in the region bounded by the restricted flow zone, which may be perceived by

the hardness color maps. These maps allow identification of zones affected by the material's flow induced by FSP. The hardness diagram also allowed to determine a higher hardness values zone on the advancing side, especially in the right lower region of the processed zone. Figure 7 shows the hardness distribution histograms of the unprocessed region and the processed zone. It can be seen that, for both steels, the processed zone showed an increment in the average hardness. The hardness distribution indicated that FSP hardened the UNS 32750 more effectively. The UNS S32101 displayed a slight boost in the average hardness values and a

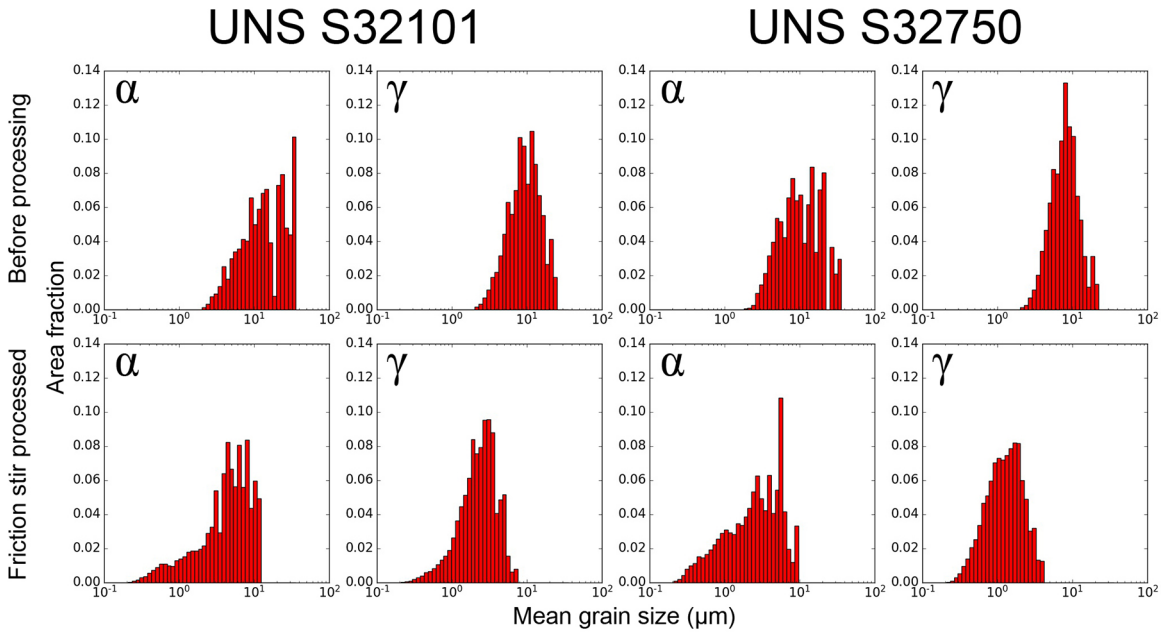


Figure 4. Mean grain size histograms of the UNS S32101 and S32750 before and after FSP. Grain size data obtained by EBSD analysis.

remarkable widening of the hardness distribution, whereas the UNS S32750 showed a considerable increase in the average hardness without a notable growth in dispersion of hardness levels. The EBSD results pointed out that FSP achieved a more intense grain refinement of both phases on UNS S32750. Moreover, this steel has a higher content of austenite, which is the phase with more effective grain refinement. These details explain the higher hardening efficiency of the UNS S32750 after FSP. Figure 8 shows the surface hardness profiles of processed and unprocessed samples for both steels. The surface hardness profiles indicated higher dispersion of values on UNS S32101 both processed and unprocessed zones. Contrarily, the S32750 also showed minor dispersion of microhardness values. The overall hardness increase on UNS S32750 was clearly higher than on UNS S32101, both for unprocessed region

(due to previous lamination process) and processed region. Table 3 contains the hardness results of both processed and unprocessed steels, indicating that average hardness values in the processed zone were 18 HV_{0.2/15} (6%) and 27 HV_{0.2/15} (8%) greater for UNS S32101 and UNS S32750, respectively. UNS S32101 showed a lower increase in average hardness due to the development of a coarser grain microstructure and also due to higher ferrite phase fraction when compared to UNS S32750. In general, higher average hardness values on processed surfaces were found compared to the average of cross-section processed zones.

3.2.2 Uniaxial tensile testing

Uniaxial tensile tests were conducted in FSP samples, the results were plotted in true strain × stress curves. Equations (1) and (2) represent the conversion from engineering strain (ϵ) to true strain (ϵ_t) and from engineering stress (σ) to true stress (σ_t), respectively.

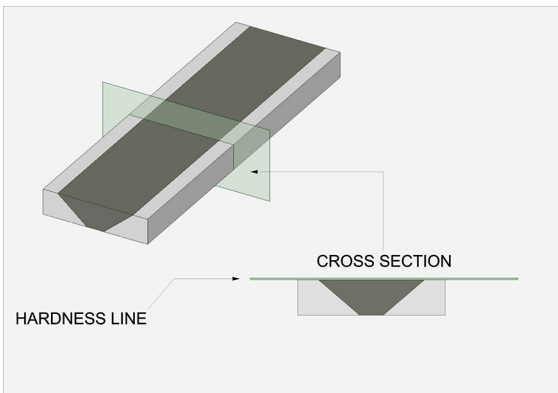


Figure 5. Schematic of regions analyzed by microhardness testing on FSP samples.

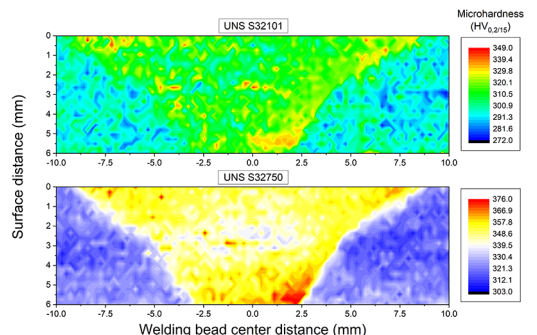


Figure 6. Hardness maps of the cross sections of FSP samples of the steels UNS S32101 and UNS S32750.

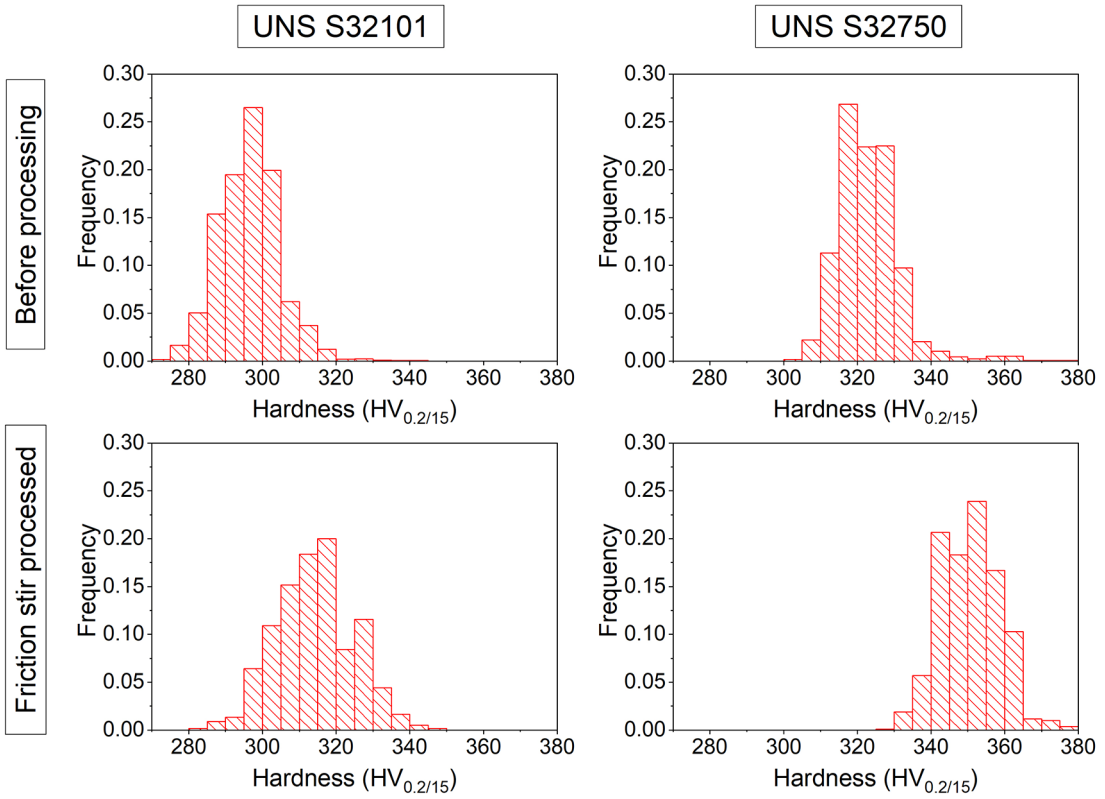


Figure 7. Histograms of Vickers microhardness distribution of the unprocessed region and the pinned friction zone of the steels UNS S32101 and UNS S32750.

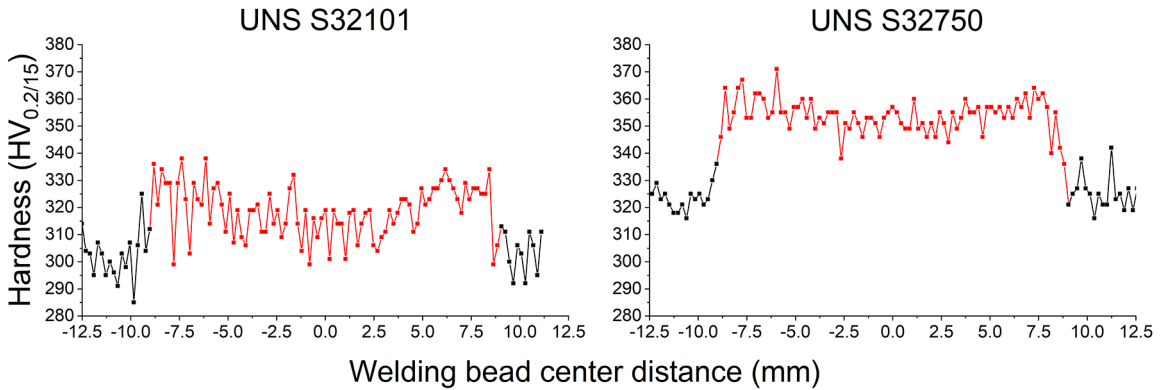


Figure 8. Hardness profiles of the friction-processed face of non-consumable pin and unprocessed region around the UNS S32101 and UNS S32750 steels.

Table 3. Descriptive statistics of the samples of Vickers microhardness measurements of the unprocessed and processed region for UNS S32101 and S32750 steels.

UNS	Condition	HV _{0.2/15}	
		Cross-section	Surface
S32101	Before processing	296 ± 8	305 ± 9
	Friction stir processed	314 ± 11	320 ± 9
S32750	Before processing	323 ± 8	326 ± 6
	Friction stir processed	350 ± 8	354 ± 6

$$\epsilon_t = \ln(1 + \epsilon) \tag{1}$$

$$\sigma_t = \sigma(1 + \epsilon) \tag{2}$$

The results of true stress × strain were used to fit a graph according to the Hollomon’s equation (3), which is correlated to a theoretical model that describes the relation between true stress and true strain in the plastic deformation. The constant *K*, called *strength coefficient*, indicates a theoretical

stress applied to the material to achieve 100% strain. The constant n , known as *Strain hardening-exponent*, is related to the work hardening propension of the material.

$$\sigma_t = K\varepsilon_t^n \quad (3)$$

Figure 9 presents the true stress *versus* strain curves for UNS S32101 and S32750 FSP samples along the respective Hollomon fitted curves. Table 4 contains the results of the fitting of experimental data to Hollomon's equation. The experimental data fitting to the Hollomon's equation indicated that UNS S32750 is briefly more prone to work hardening whereas the UNS S32101 is inclined to have a more plastic behavior. A further discussion about mechanical properties on FSP of DSS were presented by Santos et al.²⁴. Gadelrab et al.³⁰ conducted nanoindentation experiments which indicated that the elastic modulus, yield strength and hardening exponent of austenite and ferrite are statistically equivalent on DSS. The higher susceptibility of UNS S32750 to work hardening compared to S32101 is probably associated with the more effective grain refinement of the former promoted by FSP. Tavares et al. measured the work-hardening exponent for conventional duplex and lean duplex stainless steels, obtaining n results in order of 0.10³¹. Probably the substantial difference between the values measured by Tavares et al. and the values presented on occurred due the grain refinement provided by FSP.

3.3 Abrasion Test

Both unprocessed steels and FSP were submitted to rubber wheel abrasion tests to evaluate the effect of FSP on abrasive wear resistance. Figure 10 shows the schematic of the rubber wheel abrasion test samples. Figure 11 shows the result of the abrasion test by free rubber wheel particles compared to the respective sample hardness. The results indicated that the hardness increment provided decreasing abrasive wear resistance. For the UNS S32750 alloy, FSP processing resulted in greater wear rates. For the UNS S32101 the wear resistance and microhardness of the processed and unprocessed material were statistically equivalent. Nevertheless, the results pointed that an overall increase in the average hardness provides a global decrease in wear resistance. The wear resistance usually is enhanced by material hardening, however other factors influence strongly on the wear resistance, for example: the hardness ratio between the abrasive particles and the body being worn; the load that is applied by the abrasive particles into the surface; the length of the wear path; the wear mechanisms that acts on the tribosystem; the work-hardenability of the material³². Concerning the mechanical properties of the materials, one of the most common parameters that influence on abrasive wear is the plasticity, given by the relation E/H where E is the material's Young modulus and H is the material's hardness.

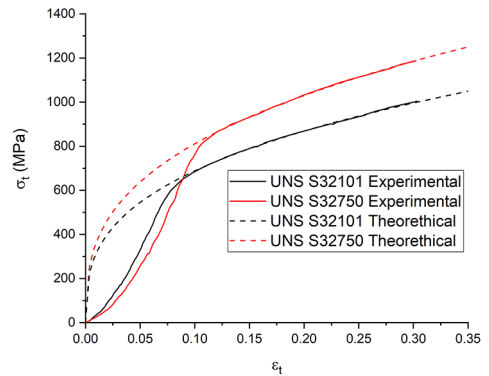


Figure 9. True stress strain curves of UNS S32101 and S32750 FSP samples along their respective Hollomon model fitted curves.

Table 4. Results of the fitted curves from experimental data to Hollomon equation.

UNS	n	K (MPa)	R ²
S32101	0.337 ± 0.001	1493 ± 2	0.99
S32750	0.344 ± 0.001	1797 ± 2	0.99

Materials with lower values of plasticity tend to present microcutting as wear mechanism and, to higher plasticity values, transition between microcutting to microcracking occurs, decreasing wear's resistance. On the other hand, materials with higher values of plasticity are prone to present microploughing as wear mechanism³². Microploughing causes reduced wear rates compared to microcutting, once that microploughing promotes more deformation than removal of material¹⁸. Another fact to highlight is the tribosystem analyzed, the abrasive's hardness is seriously higher than hardness of the worn surface. When this happens, it means that the analyzed system is subjected to severe wearing⁶. As the Young modulus is an intrinsic property of crystal structure, the E of both steels is similar, so the plasticity decreases according to the conditions presented with higher hardness values. The calculated plasticity values of the analyzed conditions were: 0.675, 0.637, 0.619 and 0.571 GPa/HV_{0.2/15}, for non-processed S32101, FSPed S32101, non-processed S32750 and FSPed S32750, respectively. These values indicated that the processed samples are more prone to action of microcutting and microcracking. For that, it is expected higher weight loss than the unprocessed ones.

The surfaces worn during the abrasion tests were analyzed by SEM to evaluate wear's micromechanisms in the tribosystem. The wear marks on the samples with and without surface treatment, for both alloys, were inspected. Figure 12 shows SEM analysis of the UNS S32101 abrasion tests worn surfaces. The SEM images indicated action of microploughing and microcutting on both processed and unprocessed samples, besides indentation marks. More plough marks were identified in unprocessed samples, opposing FSP

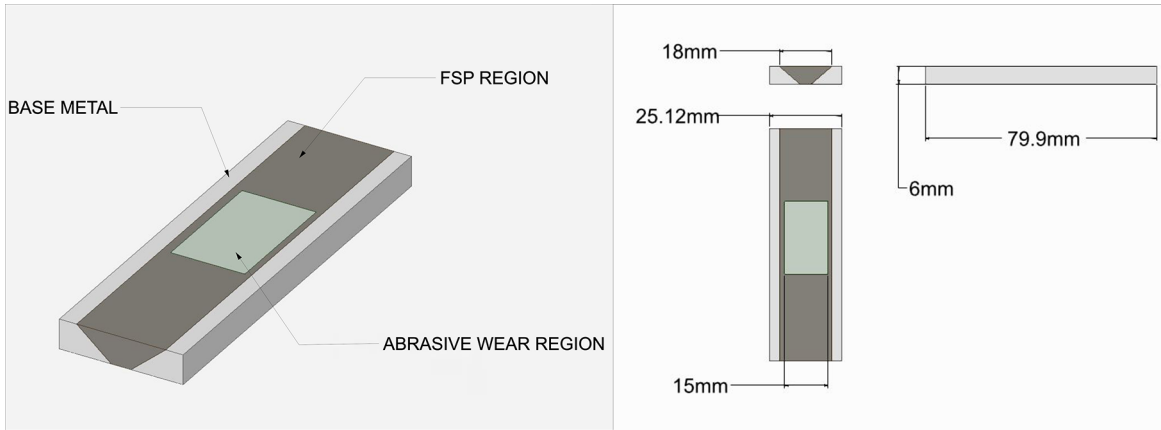


Figure 10. Schematic of the rubber wheel abrasion test samples.

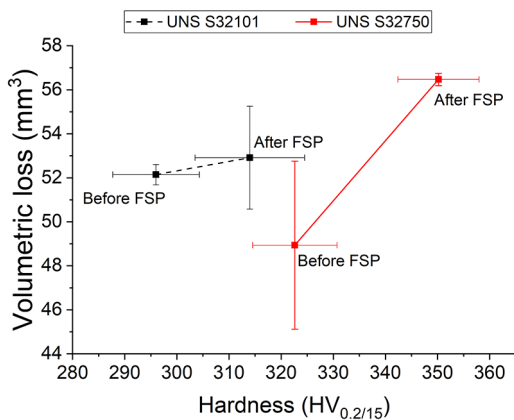


Figure 11. Results of volumetric material loss during the rubber wheel abrasion tests compared to the respective sample hardness.

samples which showed simultaneously microcutting and few microploughing shallow marks. Figure 13 displays SEM analysis of the UNS S32750 abrasion tests worn surfaces. The analysis of worn surface of UNS S32750 indicated that the unprocessed steel presented microploughing, whereas this wear mechanism was observed to be significantly less present in processed samples. Pits and cracks were observed in processed samples of both steels. The presence of pits on worn surfaces might be an microcracking indication³². Although microcracking frequently occurs in materials with low workability, rolling and indentation, caused by abrasive particles, can promote superficial fatigue of the workpiece in three-body abrasion tribosystems. Additionally, the material's subsurface is also subjected to the same mechanism, since rolling promotes higher stress on regions below the workpiece surface. In this case, the material's fatigue during wear action promotes the evolution of microcracking, leading to mass loss³³⁻³⁶. A clear evidence of the fatigue phenomenon can be the presence of pits on wear paths of FSPed samples, some of these pits are indicated by arrows in Figures 12 and 13. These pits are a result of microcracking propagation from the internal domain to

the FSPed surfaces. Pitting and microcracking formation during abrasive wear is frequently found to occur in various interfaces, such as matrix's interface³⁶ and between coatings and its original substrate³³. This characteristic then makes the friction-processed region of duplex stainless steels more prone to formation of these defects, since grain refinement promoted by friction processing favors an increase in the specific surface of α/γ interfaces. With continuous stress loading, these discontinuities propagate³⁵, causing material removal due to delamination. It is noteworthy that pitting formation is usually more evident during the early stages of abrasive wear³⁴, presenting pronounced volume loss with its formation³³.

The microploughing appeared to act significantly less frequent on UNS S32750 FSP samples compared to all the other conditions analyzed in this work, which could be an evidence that with the increasing in hardness the transition from microploughing to microcutting caused decreasing in wear resistance³². Comparing the non-processed samples of UNS S32101 and S32750 was perceptible that microploughing and microcutting was the main wear mechanism for both alloys. The higher wear resistance of S32750 unprocessed sample occurred because there was no change on wear mechanism comparing with non-processed S32101. Due to this fact, the typical behavior of hardening promoting wear resistance was identified. The FSPed samples of both steels showed few microploughing evidence, along with low number of cracks and pits, pointing that hardening of samples promoted higher wear, since the material has become more prone to fatigue.

The presented results pointed that FSP promoted alterations of wear micromechanism, boosting workpiece's wear, from microploughing and microcutting in unprocessed samples to include microcracking in FSPed samples. The grain refinement promotes hardening of the material, making it more prone to microfatigue, which favored microcracking during three-body abrasion. The results pointed that FSP of

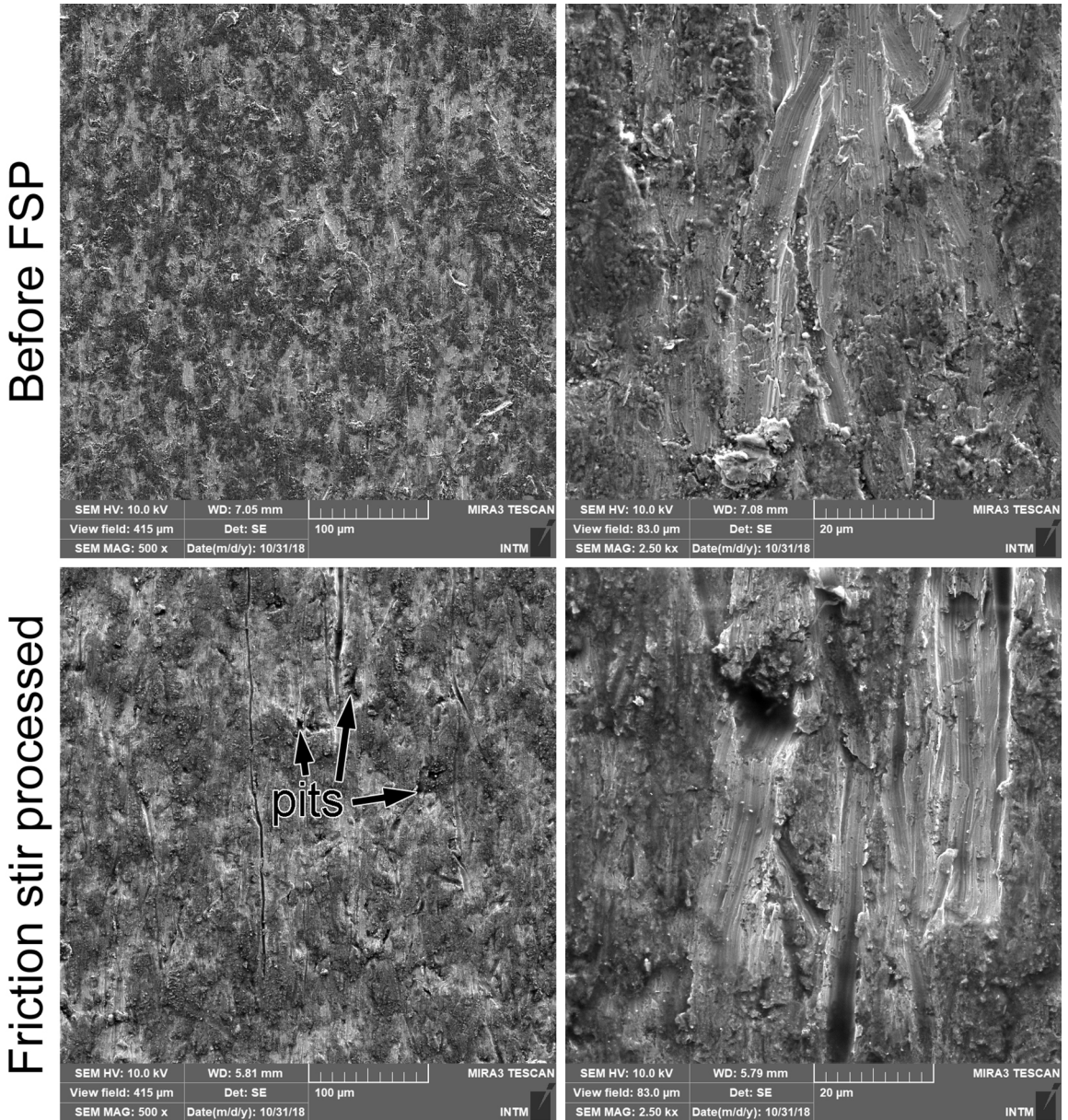


Figure 12. SEM images of worn surfaces of UNS S32101 abrasion tested surfaces.

DSS can promote reduction of its wear resistance, due the higher susceptibility of material to fatigue caused by the tribological phenomena. Thus, FSP may not be an adequate processing technology to promote enhancement of abrasive wear resistance of DSS. Once the material develops higher strain hardening levels, it tends to strongly resist against straining, which contributes to the shifting from microploughing to microcutting mechanism.

4. Conclusion

FSP was successfully employed to surface processing of both UNS S32101 and UNS S32750. EBSD analyses of processed and unprocessed samples indicated the ferrite volume fraction

remained approximately equivalent and secondary phases were not detected on processed microstructure. Grain refinement was more intense for both phases of UNS S32750. For both studied steels, austenite phase presented more intense grain refining. Microhardness values showed that, for both steels, the processed zone had an increment in the average hardness. The hardness distribution indicated that FSP hardened the UNS S32750 more effectively. UNS S32101 showed a lower increase in average hardness due to the development of a coarser grain microstructure and also higher ferrite phase fraction when compared to UNS S32750. Additionally, for both alloys an overall higher average hardness values on processed surfaces were found compared to the average of cross-section processed zones. Tensile tests results were fitted into Hollomon's equation

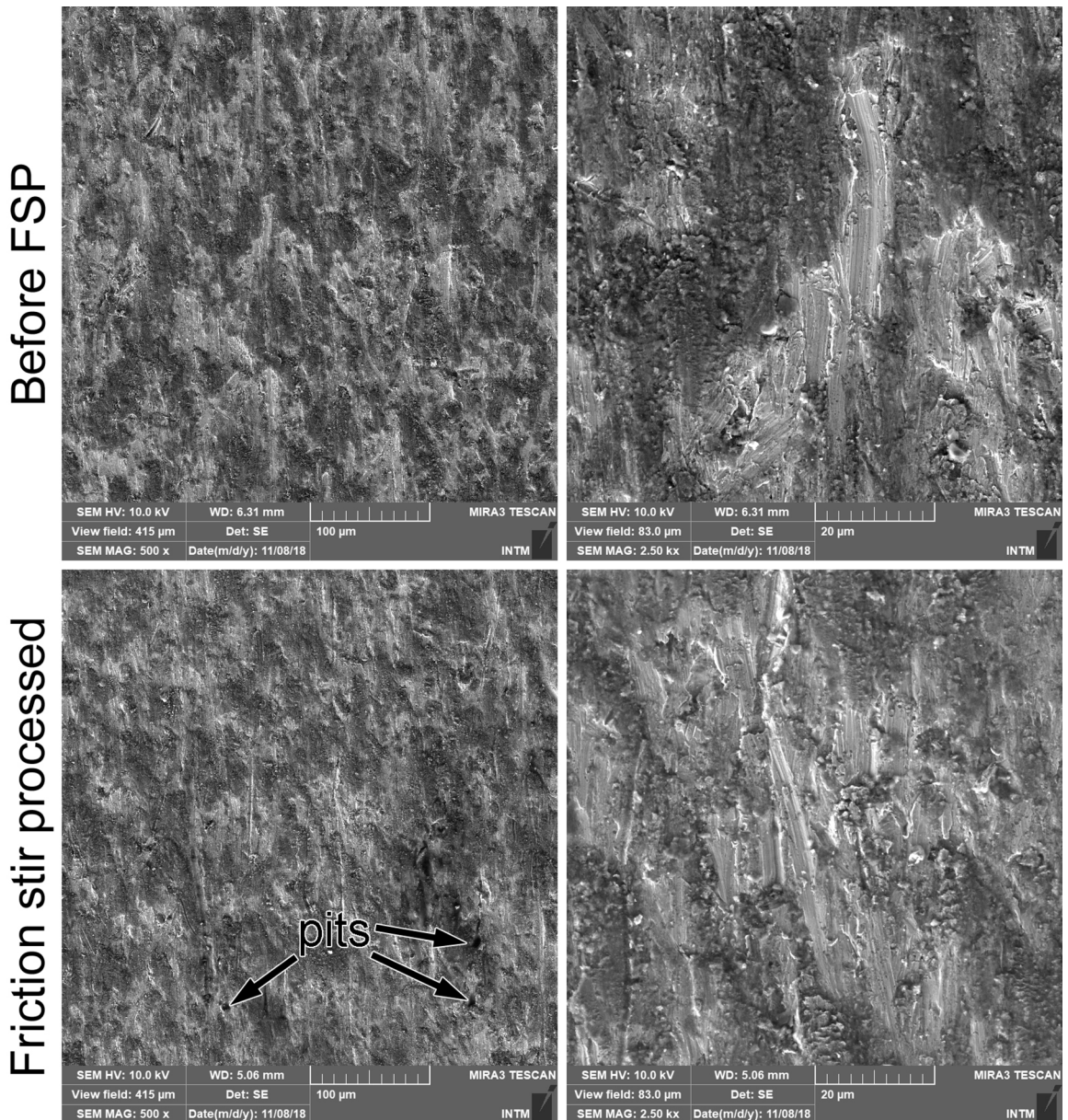


Figure 13. SEM images of worn surfaces of UNS S32750 abrasion tested surfaces.

curve and indicated that UNS S32750 is briefly more prone to work hardening whereas the UNS S32101 is inclined to have a more plastic behavior, and indicated that FSP samples presented higher propension to work-hardening compared to results of the literature. Abrasion tests results for the UNS S32750 alloy indicated that FSP resulted in greater wear rates, whereas for the UNS S32101 the wear resistance of the processed and unprocessed material was statistically equivalent. Results pointed that an overall increase in the average hardness provides a global decrease in wear resistance. The SEM images indicated action of microploughing and microcutting on both processed and unprocessed samples of UNS S32101, being microploughing prevalent in both conditions. For the UNS S32750 SEM images indicated predominant microploughing

on unprocessed samples, whereas a notable predominance of microcutting action on FSP samples was observed. These facts point out that FSP has promoted alterations of wear micromechanism from microploughing to microcutting on DSS, probably promoted by the increased work-hardening propension. The findings of this work indicate that FSP may not be a satisfactory processing technique to enhance the abrasive wear resistance of DSS.

5. Acknowledgements

The authors thank CAPES, CNPq, FACEPE, FINEP, ANP for scholarships and financial support, and Outokumpu for providing the studied materials.

6. References

- Guo Y, Hu J, Li J, Jiang L, Liu T, Wu Y. Effect of annealing temperature on the mechanical and corrosion behavior of a newly developed novel lean duplex stainless steel. *Materials (Basel)*. 2014;7(9):6604-19.
- Zhang L, Zhang W, Jiang Y, Deng B, Sun D, Li J. Influence of annealing treatment on the corrosion resistance of lean duplex stainless steel 2101. *Electrochimica Acta*. 2009;54(23):5387-92.
- McGuire MF. *Stainless steels for design engineers*. Materials Park, Ohio: ASM International; 2008.
- Boillot P, Peultier J. Use of stainless steels in the industry: recent and future developments. *Procedia Engineering*. 2014;83:309-21.
- Ilman MN, Kusmono K. Analysis of internal corrosion in subsea oil pipeline. *Case Studies in Engineering Failure Analysis*. 2014;2(1):1-8.
- Hutchings I, Shipway P. *Tribology: friction and wear of engineering materials*. 2nd ed. Cambridge, MA: Butterworth-Heinemann; 2017.
- Dallmann J. *Projeto, construção e validação de um abrasômetro roda de borracha [dissertação]*. Joinville (SC): Universidade do Estado de Santa Catarina - UDESC; 2012.
- Marques F, Silva WM, Pardal JM, Tavares SSM, Scandian C. Influence of heat treatments on the micro-abrasion wear resistance of a superduplex stainless steel. *Wear*. 2011;271(9-10):1288-94.
- Lim H, Kim P, Jeong H, Jeong S. Enhancement of abrasion and corrosion resistance of duplex stainless steel by laser shock peening. *Journal of Materials Processing Technology*. 2012;212(6):1347-54.
- Escobar JD, Velásquez E, Santos TFA, Ramirez AJ, López D. Improvement of cavitation erosion resistance of a duplex stainless steel through friction stir processing (FSP). *Wear*. 2013;297(1-2):998-1005.
- Padhy GK, Wu CS, Gao S. Friction stir based welding and processing technologies - processes, parameters, microstructures and applications: a review. *Journal of Materials Science and Technology*. 2018;34(1):1-38.
- Li K, Liu X, Zhao Y. Research status and prospect of friction stir processing technology. *Coatings*. 2019;9(2):129.
- Santos TFA, Torres EA, Lippold JC, Ramirez AJ. Detailed microstructural characterization and restoration mechanisms of duplex and superduplex stainless steel friction-stir-welded joints. *Journal of Materials Engineering and Performance*. 2016;25(12):5173-88.
- Węglowski MS. Friction stir processing – State of the art. *Archives of Civil and Mechanical Engineering*. 2018;18(1):114-29.
- Rathee S, Maheshwari S, Siddiquee AN. Issues and strategies in composite fabrication via friction stir processing: a review. *Materials and Manufacturing Processes*. 2018;33(3):239-61.
- Gandra J, Krohn H, Miranda RM, Vilaça P, Quintino L, Santos JF. Friction surfacing—a review. *Journal of Materials Processing Technology*. 2014;214(5):1062-93.
- Padhy GK, Wu CS, Gao S. Auxiliary energy assisted friction stir welding – status review. *Science and Technology of Welding and Joining*. 2015;20(8):631-49.
- Kumar S. Ultrasonic assisted friction stir processing of 6063 aluminum alloy. *Archives of Civil and Mechanical Engineering*. 2016;16(3):473-84.
- Kumar S, Wu CS, Padhy GK, Ding W. Application of ultrasonic vibrations in welding and metal processing: A status review. *Journal of Manufacturing Processes*. 2017;26:295-322.
- Mishra RS, Ma ZY. Friction stir welding and processing. *Materials Science and Engineering: R: Reports*. 2005;50(1-2):1-78.
- Santos TFA, Torres EA, Ramirez AJ. Soldagem por atrito com pino não consumível de aços inoxidáveis duplex. *Soldagem e Inspeção*. 2016;21(1):59-69.
- Santa-Cruz LA, Marques IJ, Urtiga Filho SL, Hermenegildo TFC, Santos TFA. Corrosion evaluation of duplex and superduplex stainless steel friction stir welds using potentiodynamic measurements and immersion tests in chloride environments. *Metallography, Microstructure, and Analysis*. 2019;8(1):32-44.
- Santa-Cruz LA, Machado G, Vicente AA, Hermenegildo TFC, Santos TFA. Effect of high anodic polarization on the passive layer properties of superduplex stainless steel friction stir welds at different chloride electrolyte pH values and temperatures. *International Journal of Minerals, Metallurgy, and Materials*. 2019;26(6):710-21.
- Santos TFA, López EAT, Fonseca EB, Ramirez AJ. Friction stir welding of duplex and superduplex stainless steels and some aspects of microstructural characterization and mechanical performance. *Materials Research*. 2016;19(1):117-31.
- Marques IJ, Silva FJ, Santos TFA. Rapid precipitation of intermetallic phases during isothermal treatment of duplex stainless steel joints produced by friction stir welding. *Journal of Alloys and Compounds*. 2020;820:153170.
- Atapour M, Sarlak H, Esmailzadeh M. Pitting corrosion susceptibility of friction stir welded lean duplex stainless steel joints. *International Journal of Advanced Manufacturing Technology*. 2016;83(5-8):721-8.
- Hajian M, Abdollah-Zadeh A, Rezaei-Nejad SS, Assadi H, Hadavi SMM, Chung K, et al. Improvement in cavitation erosion resistance of AISI 316L stainless steel by friction stir processing. *Applied Surface Science*. 2014;308:184-92.
- Tinubu OO, Das S, Dutt A, Mogonye JE, Ageh V, Xu R, et al. Friction stir processing of A-286 stainless steel: microstructural evolution during wear. *Wear*. 2016;356-357:94-100.
- Bachmann F, Hielscher R, Schaeben H. Texture Analysis with MTEX – Free and Open Source Software Toolbox. *Solid State Phenomena* [Internet]. 2010; [cited 2018 dec 08]; 160:63-8;. Available from: <https://www.scientific.net/SSP.160.63>
- Gadelrab KR, Li G, Chiesa M, Souier T. Local characterization of austenite and ferrite phases in duplex stainless steel using MFM and nanoindentation. *Journal of Materials Research*. 2012;27(12):1573-9.

31. Tavares SSM, Pardal JM, Abreu HFG, Nunes CS, Silva MR. Tensile properties of duplex UNS S32205 and lean duplex UNS S32304 steels and the influence of short duration 475 °C aging. *Materials Research*. 2012;15(6):859-64.
32. Gahr KHZ. *Microstructure and wear of materials*. Amsterdam: North Holland; 2010.
33. Bull SJ, Rickerby DS, Robertson T, Hendry A. The abrasive wear resistance of sputter ion plated titanium nitride coatings. *Surface and Coatings Technology*. 1988;34(3-4):743-54.
34. Boas M, Bamberger M. Low load abrasive wear behaviour of plasma spray and laser-melted plasma coatings. *Wear*. 1988;126(2):197-210.
35. Luo Q, Xie J, Song Y. Effects of microstructures on the abrasive wear behaviour of spheroidal cast iron. *Wear*. 1995;184(1):1-10.
36. Wimmer MA, Loos J, Nassutt R, Heitkemper M, Fischer A. The acting wear mechanisms on metal-on-metal hip joint bearings: in vitro results. *Wear*. 2001;250(1-12):129-39.